Fluid–solid equilibria of flexible and linear rigid tangent chains from Wertheim's thermodynamic perturbation theory

Felipe J. Blas[a)]
Departamento de Física Aplicada, Facultad de Ciencias Experimentales, Universidad de Huelva, 21071 Huelva, Spain

Eduardo Sanz and Carlos Vega
Departamento de Química Física, Facultad de Ciencias Químicas, Universidad Complutense, 28040 Madrid, Spain

Amparo Galindo
Department of Chemical Engineering and Chemical Technology, Imperial College London, South Kensington Campus, London SW7 2AZ, United Kingdom

(Received 22 July 2003; accepted 26 August 2003)

An extension of Wertheim's first-order thermodynamic perturbation theory is proposed to describe the global phase behavior of linear rigid tangent hard sphere chains. The extension is based on a scaling proposed recently by Vega and McBride [Phys. Rev. E **65**, 052501 (2002)] for the equation of state of linear chains in the solid phase. We have used the Einstein-crystal methodology, the Rahman–Parrinello technique, and the thermodynamic integration method for calculating the free energy and equation of state of linear rigid hard sphere chains with different chain lengths, including the solid–fluid phase equilibria. Agreement between the simulation data and theoretical predictions is excellent in all cases. Once it is confirmed that the proposed theory can be used to describe correctly the equation of state, free energy, and solid–fluid phase transitions of linear rigid molecules, a simple mean-field approximation at the level of van der Waals is included to account for segment–segment attractive interactions. The approach is used to determine the global phase behavior of fully flexible and linear rigid chains of varying chain lengths. The main effect of increasing the chain length in the case of linear rigid chains is to decrease the fluid densities at freezing, so that the triple-point temperatures increase. As a consequence, the range of temperatures where vapor–liquid equilibria exist decreases considerably with chain length. This behavior is a direct result of the stabilization of the solid phase with respect to the liquid phase as the chain length is increased. The vapor–liquid equilibria are seen to disappear for linear rigid chains formed by more than 11 hard sphere segments that interact through an attractive van der Waals mean-field contribution; in other words, long linear rigid chains exhibit solid–vapor phase behavior only. In the case of flexible chains, the fluid–solid equilibrium is hardly affected by the chain length, so that the triple-point temperature reaches quickly an asymptotic value. In contrast to linear rigid chains, flexible chains present quite a broad range of temperatures where vapor–liquid equilibria exist. Although the vapor–liquid equilibria of flexible and linear rigid chain molecules are similar, the differences in the type of stable solid they form and, more importantly, the differences in the scaling of thermodynamic properties with chain length bring dramatic differences to the appearance of their phase diagrams. © *2003 American Institute of Physics.* [DOI: 10.1063/1.1619936]

I. INTRODUCTION

During the last two decades, considerable advance has been achieved in understanding and predicting phase diagrams of model molecular systems.[1] The development of new and more accurate statistical mechanics methods, and the increased use of computer simulation techniques, have provided an in-depth understanding, from a molecular perspective, of the phase behavior of systems as complex as associating substances, molecules that exhibit liquid-crystalline phases, charged molecules, and molecular chains. Unfortunately, most of the theoretical studies carried out during the last years have been concerned with the thermodynamic description of the fluid (liquid and gas) phases, whereas little attention has been paid to the solid phase.[2]

From the point of view of molecular simulations, partially due to the increased speed of computers, the calculation of the complete phase diagram of a given molecular model can now be carried out within a reasonable amount of time. Although brute-force computational power is essential from a numerical perspective, the success of simulation studies is also due to the development of techniques for the calculation of phase equilibria.[3–9]

From a theoretical point of view, the understanding of the thermodynamics and phase behavior of molecular and chainlike fluids at a microscopic level has experienced an

[a)]Author to whom correspondence should be addressed. Fax: +34 959 019777; Electronic mail: Felipe.Jimenez@dfaie.uhu.es

enormous advance since late 1980s following the development of Wertheim's thermodynamic perturbation theory (TPT) for associating hard spherical fluids.[10–14] In addition, this theoretical framework, also known as the basis for the statistical associating fluid theory (SAFT) in the chemical engineering community,[15–17] provides the Helmholtz free energy, and the equation of state (EOS), of fully flexible chains of tangent spherical monomers. At the first order of approximation (TPT1) the key point of the approach is that it concludes that all the thermodynamic properties of a chain system can be obtained from knowledge of the Helmholtz free energy and the pair radial distribution function of the spherical (monomeric) reference fluid alone. A second important advantage of the theory of Wertheim is its wide range of applicability to different potential models, including Lennard-Jones,[18–22] square-well,[23,24] and Yukawa,[25] intermolecular potentials. We recommend the excellent reviews of Müller and Gubbins[26,27] of the SAFT approach for further details.

Recently, the theory of Wertheim has been extended by Vega and MacDowell[28] to describe the fluid–solid phase behavior of fully flexible tangent hard sphere chains. The theoretical predictions are in excellent agreement with the computer simulation results of Malanoski and Monson.[29] In a fully flexible tangent chain model the pair potential between monomers that form the molecules (either in the same or in different chains) is given by a spherical potential (the hard sphere potential in this work, but the discussion is also valid for other spherical intermolecular potentials, such as the Lennard-Jones potential), with no bending or torsional potentials between the monomers forming the chain (although there is an intramolecular pair interaction between monomers of the same chain separated by more than one bond). More recently, the theory has also been extended to deal with different fully flexible molecular models.[30–34] Agreement between computer simulation and theoretical predictions, not only for the EOS of chains in the solid phase, but also for the free energies in the solid phase, shows that Wertheim's perturbation theory constitutes a unified theoretical framework for describing the phase behavior (including the solid phase) of fully flexible tangent chain models.

The fully flexible chain model exhibits peculiar features in the solid phase that should be discussed at this stage. As previously mentioned, a flexible chain model has neither bending nor torsional potentials between the monomers in a chain. Therefore there is no energetic penalty when the atoms of the chains adopt a close packed structure (such as the face-centered-cubic or fcc close-packed structure) in which there is an ordered arrangement of atoms, but no long-range orientational order of chain bond vectors.[28–30] This structure is referred to as the disordered solid. Wojciechoswski *et al.*[35,36] were the first to realize that it is likely that ordered structures, such as those formed by layers of oriented molecules, do not correspond to the stable solid phases of fully flexible tangent chains. The same idea has been demonstrated by Malanoski and Monson,[29] who have determined the EOS and free energies, including the fluid–solid equilibria, of fully flexible tangent hard sphere chains with different chain lengths. The predictions of Vega and MacDowell[28] with the extension of the theory of Wertheim for the solid phase of chain molecules are in excellent agreement with their simulation data.

Although it is clear from the previous discussion that the stable solid phase of the fully flexible tangent chain model is a disordered structure, an important question arises when comparing the ordered and disordered solid structures of fully flexible chains: Why is the stable solid phase for this model the disordered one? Although the intermolecular interactions provide similar values of the free energy in both systems, an additional term associated with the degeneracy that arises from the number of ways of arranging fully flexible chains in a disordered solid provides a positive entropic contribution in the case of the flexible chains.[29] This additional term to the free energy, which can be viewed as a stabilizing effect on the solid phase of the system, lowers the free energy of the disordered structure with respect to that of the ordered solid. Obviously, the entropic contribution does not exist in an ordered solid since there is only one way to accommodate them in the ordered structure.

Another model system of chain molecules, which is similar to the previous one, but exhibits a very different stable solid structure, is the so-called linear tangent hard sphere (LTHS) chain model. As in the flexible model, the pair potential between monomers forming the linear chains (belonging either to the same chain or to different chains) is given by the hard sphere potential, but now the bond length, bond angles, and internal degrees of freedom are fixed. It is important to notice that the Hamiltonian of a system of fully flexible chains and that corresponding to linear rigid chains are different. Also, in the first model the molecules can adopt any bond angle or torsional state, as corresponds to flexible molecules, whereas these degrees of freedom are frozen in the linear rigid chain. At the first-order approximation (TPT1), Wertheim's theory does not distinguish between fully flexible and linear rigid chains;[14,15] it predicts the same EOS for both models. This surprising result, supported by computer simulation data,[37] holds very well in the fluid phase of hard sphere chains. However, this is not longer true for solid phases, as has been demonstrated recently by Vega and co-workers. Vega *et al.*[38] have performed Monte Carlo simulations and determined the EOS of LTHS chains of different chain lengths. They have found that the EOS of this model differs considerably from that corresponding to fully flexible chains. It is important to recall here another crucial difference between the models: Whereas the linear rigid chain model exhibits liquid-crystalline phases for chain lengths equal or larger than five segments, the fully flexible model presents only isotropic liquid phases. These results have been corroborated more recently by Sanz *et al.*,[31] who have performed Monte Carlo simulations in the solid phase to determine the EOS of fully flexible and linear rigid Lennard-Jones chains.

The differences between the Hamiltonians corresponding to fully flexible and linear rigid chains are responsible for the different solid structures exhibited by both of models: While the stable structure of fully flexible chains corresponds to a disordered solid, it is expected that the stable solid structure

of LTHS chains would be given by layers of molecules with the chains adopting an ordered configuration in which all molecules within the same layer point in the same direction. Examples of such structures have been proposed previously in the literature for different molecular systems.[31,39–41]

Although the stable solid configuration for a system of LTHS chains is known and well understood, little work has been devoted to study the fluid–solid phase behavior of this model. Since Wertheim's first-order perturbation theory predicts the same thermodynamic properties for fully flexible and linear rigid chains, it is obvious that in its current form the approach would not be able to predict the differences between the thermodynamic properties of the two models in the solid phase. In order to explain the differences between flexible and linear rigid chains in the solid phase Vega and McBride[42] proposed a scaling relationship for the compressibility factor of both models. The derivation used by Vega and McBride was rather heuristic, so that it is not completely satisfactory from a theoretical point of view. However, the scaling relationship was found to hold quite well in the solid phase when compared with simulation results of flexible and linear rigid chains in the solid phase.

The goal of this work is to use the scaling proposed by Vega and McBride[42] for the compressibility factor and, more importantly, to extend it to describe the free energy of the solid phase. The extension of the scaling to the free energies of the solid will allow for the first time to estimate the fluid–solid equilibrium of linear tangent hard chains from a theoretical basis. Following the well-known approach of Longuet-Higgins and Widom[43] (this seminal paper has been reprinted recently[44]) also used by Paras *et al.*[45] and by us in a previous work,[33] a segment–segment mean-field attractive contribution is incorporated both in the fluid and solid phases. The addition of a mean-field term to an accurate molecular theory yields a simple and tractable formalism and, at the same time, allows to us determine not only the liquid–solid equilibria, but also the vapor–liquid and vapor–solid phase behavior. Obviously, and due to the crude nature of the mean-field approximation, only a qualitative understanding of the phase diagram can be obtained in such a way. In this work we also address several questions involving the solid phases: do LTHS chains present a large fluid range (as seen in the case of fully flexible chains)? Would the triple-point temperatures of infinitely long rigid chains reach an asymptotic limit as that exhibited by fully flexible chains?

The scheme of this paper is as follows: In Sec. II the chain models are considered and the extension of Wertheim's theory to study the solid phase of fully flexible and linear rigid chains is described. Simulation details are reported in Sec. III. In Sec. IV the results for hard chains with attractive interactions at the mean-field level of van der Waals are given, and in Sec. V the conclusions are presented.

II. MODELS AND THEORY

In this work we shall consider two molecular models of chains: fully flexible and linear rigid tangent hard sphere chains. In the first model, the chains are flexible (i.e., there is no restriction in either the bonding angles or in the torsional angles), so that each monomer of a certain chain interacts with all other monomers in the system [i.e., in the same molecule or in other molecules with the only exception of the monomer(s) to which it is bonded] with the hard sphere potential $u^{\mathrm{ref}}(r)$. In the second model, the interactions between segments are identical to those in the fully flexible model (i.e., the spherical segments interact through the hard sphere potential), but as the chains are rigid, intramolecular interactions (interactions between segments in the same molecule) are now irrelevant since contribution to the Hamiltonian of the system is simply a constant.

A. Brief description of Wertheim's thermodynamic perturbation theory

Consider a system of chains of m tangent spherical segments (monomers), at a volume V and temperature T. The spherical segments interact through a pair potential $u^{\mathrm{ref}}(r)$; in this work, we focus on spherical segments modeled as hard spheres of diameter σ, so that $u^{\mathrm{ref}}(r)$ is given by the hard sphere potential. The molecules are modeled as tangent chains so that each monomer of a certain chain interacts with all other monomers in the system [i.e., in the same molecule or in other molecules with the only exception of the monomer(s) to which it is bonded] with the pair potential $u^{\mathrm{ref}}(r)$. The Helmholtz free energy of tangent hard sphere chains, A, can be written as[14,15,19]

$$\frac{A}{Nk_BT}=\frac{A^{\mathrm{ideal}}}{Nk_BT}+m\frac{A_r^{\mathrm{ref}}}{N^{\mathrm{ref}}k_BT}-(m-1)\ln y^{\mathrm{ref}}(\sigma), \tag{1}$$

where N is the number of chain molecules, k_B is Boltzmann's constant, A^{ideal} is the Helmholtz free energy of an ideal system of tangent chains given by $Nk_BT\{\ln(\rho\sigma^3)-1\}$ (by setting the de Broglie wavelength equal to σ), A_r^{ref} is the residual free energy of the reference system formed by $N^{\mathrm{ref}}=Nm$ hard sphere molecules, and $y^{\mathrm{ref}}(\sigma)$ is the background correlation function of the reference system at contact length. Note that in the case of monomers tangentially bonded, $y^{\mathrm{ref}}(\sigma)=g^{\mathrm{ref}}(\sigma)$, where $g^{\mathrm{ref}}(\sigma)$ is the pair radial distribution function at contact length. The EOS of the chain system, Z, which can be derived from Eq. (1), is given by

$$Z=mZ^{\mathrm{ref}}-(m-1)\left\{1+\rho^{\mathrm{ref}}\frac{\partial \ln y^{\mathrm{ref}}(\sigma)}{\partial\rho^{\mathrm{ref}}}\right\}, \tag{2}$$

where Z^{ref} is the compressibility factor of the reference system and ρ^{ref} is the number density of hard spheres, related to the density of chains through $\rho^{\mathrm{ref}}=m\rho$. We denote Eqs. (1) and (2) as Wertheim's TPT1 (Refs. 15 and 19).

B. Fluid phase description for flexible and linear rigid chains

It is well known that Wertheim's TPT1 can be used to predict accurately the thermodynamic phase behavior of hard sphere chains in the fluid phase. In particular, at the first level of approximation the theory does not distinguish between fully flexible and linear rigid chains, and therefore it predicts the same EOS for a fully flexible chain and for a fully rigid chain. This surprising result holds very well for the fluid phase of hard sphere chains.[37]

In this work we use Wertheim's TPT1[14,15,19] approach to describe the fluid phase behavior of both fully flexible and linear rigid tangent chains. As mentioned in the previous section, in order to use the theory to predict the thermodynamic properties of the fluid phase of both models, a knowledge of the residual free energy of the monomer hard sphere system and of its pair radial distribution function at contact length are required. Here we give only a short summary of the main expressions.

The Carnahan–Starling EOS[46]

$$Z_f^{\mathrm{ref}}=\frac{1+\eta+\eta^2-\eta^3}{(1-\eta)^3} \tag{3}$$

is used to describe the compressibility factor of the hard sphere system in the fluid phase. Here η represents the packing fraction of hard spheres, defined in the usual way,

$$\eta=\frac{\pi}{6}\sigma^3\rho^{\mathrm{ref}}=\frac{\pi}{6}\sigma^3 m\rho. \tag{4}$$

The residual Helmholtz free energy of the system in this phase can be easily obtained from Eq. (3) by thermodynamic integration: i.e.,

$$\frac{A_{r,f}^{\mathrm{ref}}(\eta)}{N^{\mathrm{ref}}k_BT}=\int_0^{\eta}\frac{(Z_f^{\mathrm{ref}}-1)}{\eta}d\eta. \tag{5}$$

The virial route can be used to obtain the pair radial distribution function of the system contact length,

$$Z_f^{\mathrm{ref}}=1+4\eta g_f^{\mathrm{ref}}(\sigma), \tag{6}$$

where $g_f^{\mathrm{ref}}(\sigma)$ is the pair radial distribution function of the reference system at contact length in the fluid phase.

Wertheim's TPT1 predictions from Eqs. (1) and (2) for both fully flexible and linear rigid tangent chains in the fluid phase can be obtained using Eqs. (3), (5), and (6).

C. Solid phase description for fully flexible chains

Recently, Vega and MacDowell[28] have demonstrated the possibility of extending Wertheim's perturbation theory to deal with solid phases of fully flexible hard sphere chains by noting that the arguments used to arrive to Wertheim's TPT1 equations make no special mention of the actual nature of the phase considered. The same is true for Lennard-Jones chains,[30,31,34] fully flexible hard disk chains,[32] and fully flexible hard chain molecules with segment–segment interactions treated at the mean-field level of van der Waals.[33] In summary, in order to use Wertheim's theory to predict the thermodynamic properties of the solid phase of fully flexible chains, only the residual free energy and the pair radial distribution function at contact length of the reference hard sphere system in the solid phase are required. Expressions for these properties have been presented in detail elsewhere;[28,33] here, we give a short summary of the main expressions. The residual free energy of the reference hard sphere monomer in the solid phase, $A_{r,s}^{\mathrm{ref}}$, can be obtained from the following equation:

$$\frac{A_{r,s}^{\mathrm{ref}}}{N^{\mathrm{ref}}k_BT}=5.91889+\int_{0.5450}^{\eta}\frac{(Z_s^{\mathrm{ref}}-1)}{\eta}d\eta. \tag{7}$$

Equation (7) uses thermodynamic integration to get the free energy of the solid phase at any volume fraction, provided that the free energy at a reference volume fraction $\eta=0.5450$ is known (its value being 5.918 89 in units of $N^{\mathrm{ref}}k_BT$). Notice that this is the best estimate currently available of the free energy of the hard sphere monomer in the solid phase.[47] All that is then needed to evaluate Eq. (7) is an expression for the EOS of the hard sphere monomer in the solid phase. The compressibility factor of the hard sphere reference system in the solid phase is well described by the EOS proposed by Hall.[48] The expression of Hall is essentially a least-squares fit to the simulation results of hard spheres obtained by Alder, and for this reason, it cannot be used for volume fractions beyond the range of the fit. For example, the equation of Hall predicts a pressure increase for decreasing densities in the case of packing fractions lower that $\eta\approx 0.46$. For this reason the Hall EOS is not recommended for packing fractions below those of the melting of hard spheres. In view of this, we have decided to use a different EOS to describe the monomer hard sphere in the solid phase. The equation should be mathematically simple and provide a reasonable description of the hard sphere solid and without pathological behavior at volume fractions lower than those of hard spheres at melting. We shall use a simple expression based on the cell theory (not the exact free volume expression of Buehler *et al.*,[49] but a simplified expression based on the smearing approximation[50,51]). The EOS that we shall use in this work for the hard sphere monomer solid is

$$Z_s^{\mathrm{ref}}=\left[1-\left(\frac{\eta}{\eta_c}\right)^{1/3}\right]^{-1}, \tag{8}$$

where $\eta_c=\pi\sqrt{2}/6$ is the volume fraction of hard spheres at close packing. The performance of Eq. (8) has been presented in Ref. 51 and it is seen to perform reasonably well. The pair radial distribution function of the reference system in the solid phase at contact length, $g_s^{\mathrm{ref}}(\sigma)$, can be obtained using the virial route,

$$Z_s^{\mathrm{ref}}=1+4\eta g_s^{\mathrm{ref}}(\sigma). \tag{9}$$

D. Solid phase description of linear rigid chains

It is clear that the TPT1 theory of Wertheim presented in the previous section cannot be used to describe the thermodynamic phase behavior of LTHS chains in solid phase. In principle, extensions of the theory to higher orders could be developed to deal with such chains,[14] but unfortunately, the second and higher orders of the perturbation scheme of Wertheim require the knowledge of the third-, fourth-, and higher-order distribution functions of the hard sphere reference system. Little is known about such complex functions in the solid phase, so that such extensions are not possible at the moment.

Vega and McBride[42] have recently proposed an alternative and successful procedure to use the theory of Wertheim in the context of LTHS chains in solid phase. This approach

is based on a scaling factor, which depends on the degrees of freedom of the linear rigid and fully flexible chains and which provides the pressure of rigid linear chains in terms of the pressure of fully flexible chains. If Z_{linear} is the compressibility factor of linear rigid hard sphere chains and Z_{flex} is the corresponding factor for fully flexible chains, the scaling of Vega and McBride[42] can be written as

$$Z_{\text{linear}} = \left(\frac{f_{\text{linear}}}{f_{\text{flex}}} \right) Z_{\text{flex}}, \tag{10}$$

where f_{linear} is the number of degrees of freedom of the linear rigid chains, which is equal to 5, and f_{flex} is the number of degrees of freedom of fully flexible chains, which is $3+2(m-1)$ (since the bond length of the model is fixed, f_{flex} is given by three degrees of freedom of an arbitrary atom in the model and two degrees of freedom for each of the bonds). This results in the formula

$$Z_{\text{linear}} = \left(\frac{5}{3+2(m-1)} \right) Z_{\text{flex}}. \tag{11}$$

The scaling given by Eq. (11) due to Vega and McBride shows excellent agreement with Monte Carlo simulation data[42] for LTHS chains when the properties of the flexible chain are given in the TPT1 approach. Although the authors have provided a heuristic argument within the context of the cell theory, the approach should be understood as a phenomenological rule which may help to provide an estimate of the thermodynamic phase behavior of LTHS chains in the solid phase.

Since Eqs. (10) or (11) can be used for calculating the EOS of linear rigid chains, it is natural to wonder whether it could also be used to describe the global phase behavior of linear rigid chains. Noting, in this context, that an accurate EOS does not guarantee the correct prediction of the fluid–solid equilibria, as the theoretical approach must also provide good estimates for the free energies in the solid phase. The change of free energy of LTHS chains can be computed from

$$\frac{\partial (A_{\text{linear}}/Nk_BT)}{\partial \eta} = \frac{Z_{\text{linear}}}{\eta}, \tag{12}$$

which indicates that the same scaling used in Eq. (10) or (11) can be used for the *change* of free energy of linear rigid chains. However, in order to obtain the global phase behavior of the model system, the value of the free energy (and not just its change with density) is needed.

The key point for calculating the absolute value of the free energy for linear rigid chains is directly related with the difference between the solid structures of the linear and flexible models. Fully flexible chains present configurational degeneracy in the solid phase, which is accounted for with the scaling proposed by Vega and McBride.[42] Wertheim's theory—and in particular Eq. (1)—accounts implicitly for this contribution. Such *entropic* contribution to the free energy arises from the existence of a number of ways of forming the disordered solid, whereas there is only one way of forming an ordered solid.[28,29] In other words, the configuration that minimizes the free energy of linear chains in the solid phase is expected to be unique and based on a structure of hard spheres, with the bonds of the linear molecules exhibiting long-range orientational order. Such entropic contribution must be evaluated independently and later subtracted from Eq. (1) in order to obtain a more accurate Helmholtz free energy for linear molecules.

The degeneracy contribution of the free energy associated to fully flexible chains in a disordered solid is encountered in the statistical mechanics of lattice models of polymers[52,53] and can be accurately estimated using mean-field theories, such as those of Flory[54] and Huggins,[55] which provide an estimation of the configurational degeneracy of a solution of polymers in a low-molecular-weight solvent in a lattice. The Huggins estimate,[55] which has been used previously by Malanoski and Monson,[29] is also used in this work. The contribution to the Helmholtz free energy under this approximation is given by[29,55]

$$\frac{A_{\text{deg}}}{Nk_BT} = -(m-2)\ln(z-1) - \left(1-\frac{z}{2}\right) m \ln(zm) - \left(z\frac{m}{2} - m + 1\right) \ln[zm - 2(m-1)] + \ln 2, \tag{13}$$

where z is the coordination number of the lattice, which in our case is set equal to $z=12$ for an fcc lattice. Notice that the degeneracy contribution to the free energy is negative, hence making the disordered solid phase more stable.

In summary, the Helmholtz free energy of a system of linear LTHS chain molecules can be obtained following two steps:

(i) Subtraction of the degeneracy contribution to the free energy, given by Eq. (13), from the Helmholtz free energy of fully flexible hard sphere chains of Eq. (1).

(ii) Application of the scaling of Vega and McBride, given by Eq. (11), to the result obtained in the previous step.

The final mathematical expression for A_{linear}, the Helmholtz free energy of linear rigid hard sphere chains, can be written as

$$\frac{A_{\text{linear}}}{Nk_BT} = \left(\frac{5}{3+2(m-1)} \right) \left\{ \frac{A_{\text{flex}}}{Nk_BT} - \frac{A_{\text{deg}}}{Nk_BT} \right\}. \tag{14}$$

Other thermodynamic properties can be obtained from the previous expression using standard thermodynamic relationships. In particular, the compressibility factor obtained from this equation is identical to that given by Eq. (11), since the degeneracy contribution to the free energy, A_{deg}, is independent of density.

E. Mean-field attractive interactions

A full description of the global phase behavior of molecular chains would not be complete without taking into account the attractive interactions between the segments that form the chains. These forces need to be incorporated into the model in order to study the vapor–liquid and vapor–solid phase equilibria, in addition to the solid–liquid phase behavior. As mentioned in the Introduction, we follow here the approach introduced by Longuet-Higgins and Widom[33,43,44] and add a simple mean-field term to the free energies of both

the fully flexible and LTHS chain models given by Eqs. (1) and (14), in the fluid and solid phases. We have already used this approach in a previous work.[33]

The Helmholtz free energy due to the segment–segment attractive interactions treated at the mean-field level of van der Waals is given by[15,33]

$$\frac{A^{\mathrm{mf}}}{Nk_BT} = -m\eta\left(\frac{\epsilon_{\mathrm{mf}}}{k_BT}\right), \tag{15}$$

where ϵ_{mf} is the integrated van der Waals mean-field segment–segment attractive energy.

III. SIMULATION DETAILS

The so-called close-packed structure 1 (CP1)[39] is used as the equilibrium solid structure for the linear tangent hard sphere model. In this structure the monomers of the system form an fcc close-packed arrangement of spheres at the maximum possible density. The molecules form layers and the molecular axes of all the molecules point in the same direction. A more detailed description of the structure is given in Refs. 38 and 39. Other close-packed structures of hard diatomics were described in Ref. 39, but the differences in free energy between different structures were found to be small. Similarly, we expect small differences for the thermodynamic properties of different close packed structures of the LTHS model.

Recently,[38] computer simulations for the LTHS model in the solid phase with $m=3$, 4, 5, 6 have been performed using the Rahman–Parrinello[7] modification of the constant-pressure N-P-T Monte Carlo technique in order to allow for anisotropic changes of the simulation box shape[8] since the solid CP1 structure does not have cubic symmetry. The simulation results for the equation of state were reported elsewhere.[38] In this work free energy calculations have been performed for the LTHS in the solid phase (CP1 structure) for $m=3$, 4, 6. These free energy calculations allow to determine the fluid–solid transition of the LTHS model and provide a test of the performance of the theory described in this paper. The free energies of the solid phases have been calculated using the Einstein-crystal methodology.[9,56] The method used here is quite similar to the one described in previous works.[39,57,58] The idea is to build a reversible path between the solid and an ideal Einstein crystal. In the ideal Einstein crystal the molecules are linked to the lattice sites with harmonic springs, and there are no intermolecular interactions. Translational and orientational springs are used. The maximum value of the strength of the spring $\lambda_{\max}$ used in the calculations was the same for both translational and orientational springs. We used $\lambda_{\max}=1300$, 5500, 9000 for $m=3$, 4, 6, respectively (note that the units are of k_BT/σ^2 for the translational spring and of k_BT for the orientational spring). Fifteen different values of λ in the range $0\leqslant\lambda\leqslant\lambda_{\max}$ were used to connect the reference solid to the interacting Einstein crystal. The difference in free energy between the interacting Einstein crystal and the noninteracting Einstein crystal was obtained by using umbrella sampling as described in Ref. 39. The length of the runs for the free energy calculations was 40 000 equilibration cycles +40 000 averaging cycles. In the case of the CP1 structure it is important to mention that the shape of the equilibrium unit cell at a given density is slightly different to that of close packing. The free energy calculations were carried out using the equilibrium unit cell at each density. The equilibrium shape of the unit cell was taken from our previous work (meaning that the number of particles and the arrangement of the molecules used for the free energy calculations in this work are identical to those used in Ref. 38). Once the free energy of the solid at a reference packing fraction η_0 is known, the free energies at other densities can be obtained as

$$\frac{A_s(\eta)}{Nk_BT} = \frac{A_s(\eta_0)}{Nk_BT} + \int_{\eta_0}^{\eta}\frac{Z_s}{\eta}d\eta, \tag{16}$$

where Z_s is the compressibility factor of chain molecules in the solid phase. The residual free energies of the fluid phase $A_{r,f}$ can be obtained by thermodynamic integration:

$$\frac{A_{r,f}(\eta)}{Nk_BT} = \int_0^{\eta}\frac{(Z_f-1)}{\eta}d\eta, \tag{17}$$

where Z_f is the compressibility factor of chain molecules in the fluid phase. The EOS of the fluid phase for $m=4$, 6 has been reported previously.[38] In the case of $m=3$ we perform new simulations to determine the EOS in the fluid phase. Equation (17) is integrated in the low-density region (up to volume fractions of about 0.10) using the virial expansion truncated at fourth order in density (the virial coefficients of the LTHS for $m=3$, 4, 6 were determined some time ago[59]), and for packing fractions higher than 0.10 the equation-of-state simulation results are fitted to an empirical expression.

The fluid–solid equilibria for $m=3$ and $m=4$ were obtained by equating the chemical potentials and pressures of the fluid and solid phases. We did not evaluate the fluid–solid equilibrium for $m=6$ since liquid-crystalline phases (nematic and smectic) are known[38,60] to be present between the fluid and solid phases in this case.

IV. RESULTS

We have used the expressions presented in the previous section to obtain the phase diagram of LTHS chains incorporating attractive interactions in the mean-field approximation of van der Waals. We have also determined the phase behavior of fully flexible chains, and the results corresponding to both models have been compared. The phase equilibria between two or three given phases have been calculated in the usual way, by equating the pressure and chemical potential in each phase. Throughout this section we use the integrated mean-field dispersive energy ϵ_{mf} as the unit of energy and the hard sphere diameter σ of the monomers forming the chains as the unit of length. According to this, we define the reduced temperature and pressure as $T^*=k_BT/\epsilon_{\mathrm{mf}}$ and $p^*=p\sigma^3/\epsilon_{\mathrm{mf}}$. The coexistence densities are given in terms of the packing fraction η.

Before presenting the results corresponding to the phase behavior of fully flexible and linear rigid hard sphere chains with segment–segment attractive interactions at the mean-field level of van der Waals, we examine the solid–fluid phase behavior of linear tangent hard sphere molecules of

TABLE I. Helmholtz free energies for linear rigid tangent hard sphere chains with different chain lengths corresponding to an ordered solid (labeled CP1 in Ref. 39) obtained from Einstein-crystal calculations, $A^{\text{simul}}/(Nk_BT)$, and from the extension of Wertheim's first-order thermodynamic perturbation theory, $A^{\text{theory}}/(Nk_BT)$. The density is given in terms of the packing fraction $\eta=(\pi/6)\sigma^3\rho^{\text{ref}}$.

m	η	$A^{\text{simul}}/(Nk_BT)$	$A^{\text{theory}}/(Nk_BT)$[a]	$A^{\text{theory}}/(Nk_BT)$[b]
3	0.569 45	11.770	12.382	12.359
4	0.631 13	15.165	15.686	15.880
6	0.618 42	15.378	15.861	16.011

[a]Obtained using the cell theory for the hard sphere reference system in the solid phase.
[b]Obtained using the Hall EOS for the hard sphere reference system in the solid phase.

different chain lengths. This is done by setting $\epsilon_{\text{mf}}=0$ in Eq. (15). In Table I the theoretical predictions and simulation results for the free energy of linear rigid hard sphere chains in the solid phase are presented. As can be seen, the agreement between the theory and simulation data is quite good, with deviations of about 5%. It is important to emphasize here that the theoretical determination of the free energy of linear rigid tangent hard chains in the solid phase is not an easy task, so that the accuracy of the results of Table I justify the use of the approximations leading to Eq. (14). The difference in the free energy in the solid phases of the flexible chain model and the rigid linear model can be seen by comparing the data in Table I in this work and those of Table I in Ref. 28. The comparison reveals that the free energies of flexible chains are substantially larger than those of linear rigid chains (for instance, for $m=4$ the free energy of the flexible chains is about twice that of the linear rigid chains). Moreover, the variation of the free energy of the solid phase with chain length m is markedly different for the flexible and linear rigid chains. For a given volume fraction (i.e., η) the free energy of the flexible chains in the solid phase increases linearly with m, whereas that of the linear rigid chains becomes practically independent of m for relatively small values of m (Ref. 42). Notice that in the fluid phase flexible and linear rigid chains present very similar (identical in the TPT1 approach) equations of state and free energies, which increase linearly for increasing m. Summing up, flexible and rigid hard chains present the same scaling for the free energy for the fluid phase, but different scaling for the free energy of the solid phase.[42] The freezing behavior of both systems can be expected to be rather different given the different behavior of the solid free energies in the solid phase.

In Fig. 1 the EOS for fully flexible and LTHS chains with $m=3$ are shown, including the fluid and solid phases, as well as the solid–fluid phase transition obtained from the extension of Wertheim's theory and the computer simulations of this work. We have also included the computer simulation results of fully flexible hard sphere chains of Malanoski and Monson.[29] As can be seen, the EOS of both models in the fluid phase are nearly identical, as expected. However, the EOS of fully flexible and linear rigid chains in the solid phase are dramatically different. For a given pressure, the linear rigid chains have a higher density in the solid phase

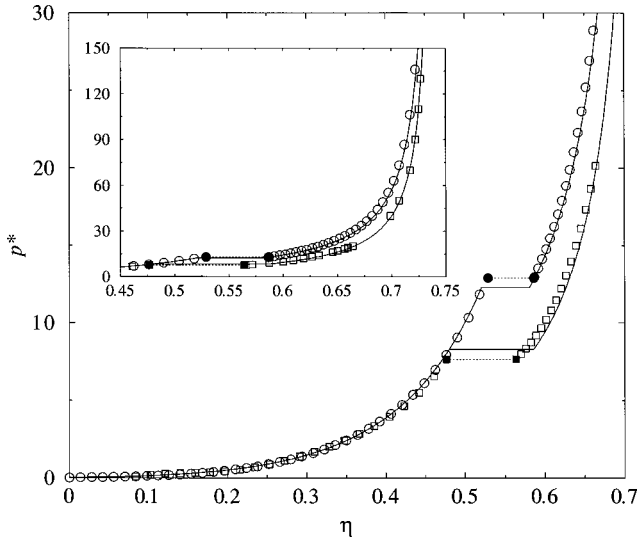

FIG. 1. EOS of fully flexible and LTHS chains with $m=3$ in the fluid and solid phases. The solid lines correspond to the theoretical predictions. The open circles represent molecular simulation results for fully flexible chains taken from the literature (Ref. 29) and the open squares the simulation data for linear rigid chains obtained in this work and taken from the literature (Ref. 38). The solid symbols with horizontal dotted lines represent the fluid–solid coexistence densities and tie lines, respectively, for flexible (circles) (Ref. 29) and linear (squares) chains obtained in this work. The horizontal solid lines represent the theoretical predictions for the transitions. The inset shows the high-pressure behavior of the EOS in the solid phase. The reduced pressure is given as $p^*=p/(k_BT)$.

than the flexible ones. Conversely, for a certain packing fraction the pressure of the flexible model is considerably higher than that of the linear rigid one. A consequence of this shifting is that the solid–fluid phase transition of linear rigid chains occurs at lower pressures than those corresponding to fully flexible chains. In Fig. 2 the fluid–solid equilibrium of flexible and linear rigid hard sphere chains with $m=4$ is presented. The trends are similar to those presented in Fig. 1 for $m=3$. Note, however, that in passing from $m=3$ to $m=4$, the freezing properties of flexible chains hardly change, whereas those of linear rigid chains undergo important changes. As can be seen, agreement between the theoretical predictions and simulation data is excellent at all thermodynamic conditions, including the solid–fluid coexisting properties. The message from Figs. 1 and 2 is that by using the EOS of hard spheres in the fluid phase and the EOS of hard spheres in the solid phase, it is possible to yield reasonable predictions of the fluid–solid equilibrium of flexible and LTHS chains. It is striking that all the information required to implement the theory was available forty years ago already.

In Table II the fluid–solid coexistence properties of linear rigid hard chains are presented. The results for the flexible chain model are also presented. It can be seen that, whereas the packing fraction of fully flexible chains at freezing remains approximately constant, that of linear rigid chains decreases as m increases. The results of Table II show that the extension of the theory of Wertheim presented in this work is able to provide an excellent description of the solid–fluid phase transition for flexible and LTHS chains, although it is important to note here that linear rigid hard chains greater than $m=5$ are known to exhibit liquid-crystalline

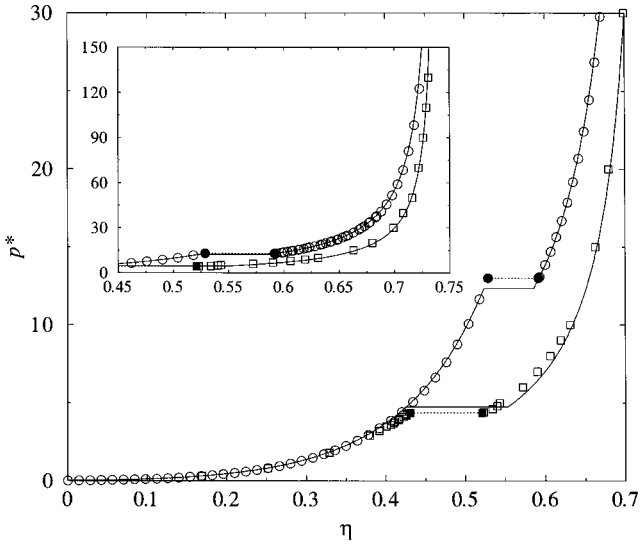

FIG. 2. EOS of fully flexible and LTHS chains with $m=4$ in the fluid and solid phases. The solid lines correspond to the theoretical predictions. The open circles represent molecular simulation results for fully flexible chains taken from the literature (Ref. 29) and the open squares the simulation data for linear rigid chains obtained in this work and taken from the literature (Ref. 38). The solid symbols with horizontal dotted lines represent the fluid–solid coexistence densities and tie lines, respectively, for flexible (circles) (Ref. 29) and linear (squares) chains obtained in this work. The horizontal solid lines represent the theoretical predictions for the transitions. The inset shows the high-pressure behavior of the EOS in the solid phase. The reduced pressure is given in as $p^*=p/(k_BT)$.

phase behavior in addition to the fluid–solid phase behavior studied in this work.

Once we have checked that the scaling proposed by Vega and McBride[42] for the EOS and the scaling proposed in this work for the Helmholtz free energy of LTHS molecules are able to predict accurately the solid–fluid phase transition for different chain lengths, we use the theory presented in Sec. II to describe the phase behavior of linear rigid chains with segment–segment attractive interactions at the mean-field level of van der Waals. We consider first the global phase behavior of fully flexible chains. In Fig. 3(a) the coexistence curves of fully flexible hard chain molecules with different chain lengths and with segment–segment attractive interactions at the mean-field level are presented. As can be seen in the T-η projection, the phase diagram of fully flexible chains is characterized by a large fluid range. In addition, the triple-point temperature reaches very rapidly an asymptotic finite value and the solid–fluid coexistence densities become similar for long chain molecules. The largest increase in the solid–fluid phase behavior occurs in going from the dimer to the trimer system. It is important to note here that the triple temperature [showed in the inset of Fig. 3(a)] is close to constant for the chain lengths considered, although it slightly increases as the chain length is larger. The results presented here using the cell theory[50,51] to describe the solid phase of the hard sphere monomer are similar to those obtained in a previous work with the EOS of Hall[48] for the hard sphere solid.[33] The p-T projection of the phase diagram and its $\log p$-T representation are presented in Figs. 3(b) and 3(c), respectively. As can be seen, the solid–liquid melting line is almost vertical, showing a small dependence on the chain length, as suggested by the previous figure, and indicating a large fluid range in all cases. The temperature dependence of the solid–vapor coexistence pressure is better seen in the $\log p$-T representation. As can be seen, the triple pressure decreases by several orders of magnitude as the chain length increases. This is in contrast with the behavior of the triple temperature, which is nearly constant for the chain lengths studied ($m=2-6$) (see Table III).

The T-η projection of the phase diagram of LTHS chains with segment–segment attractive interactions at the mean-field level is presented Fig. 4(a). Important differences with the coexistence curves of the fully flexible chain model can be observed. The most striking concerns the behavior of the solid–liquid coexistence as the chain length is increased: in the case of the fully flexible chains the equilibrium curves are practically identical (although slight density increases are seen as the chain length is increased), whereas in the case of linear rigid molecules the coexistence boundaries are greatly displaced toward lower densities as the chain length is increased, indicating that the solid phase becomes more stable than the liquid phase. A second important difference, related to the first one, is the behavior of the triple temperature, which increases for larger molecules. As a consequence of this, the liquid–vapor coexistence region becomes smaller in both the temperature and density ranges. Note that the fluid

TABLE II. Fluid–solid coexistence data for fully flexible and linear rigid chains formed by three and four tangent hard sphere segments. The simulation data have been obtained from Ref. 29 (fully flexible) and from this work (linear rigid) using the Einstein-crystal methodology for calculating the Helmholtz free energy, thermodynamic integration, and N-P-T simulations using the Rahman–Parrinello technique. The theory corresponds to the predictions from the extension of Wertheim's approach proposed in this work. The reduced pressure p^* is given by $p^*=p/(k_BT)$.

m	Model	Method	η_f	η_s	p^*
3	Fully flexible	Simulation	0.5288	0.5864	12.90
3	Fully flexible	Theory	0.5205	0.5810	12.29
4	Fully flexible	Simulation	0.5289	0.5917	13.00
4	Fully flexible	Theory	0.5236	0.5855	12.34
3	Linear rigid	Simulation	0.4764	0.5639	7.655
3	Linear rigid	Theory	0.4797	0.5861	8.296
4	Linear rigid	Simulation	0.4308	0.5209	4.367
4	Linear rigid	Theory	0.4252	0.5529	4.741

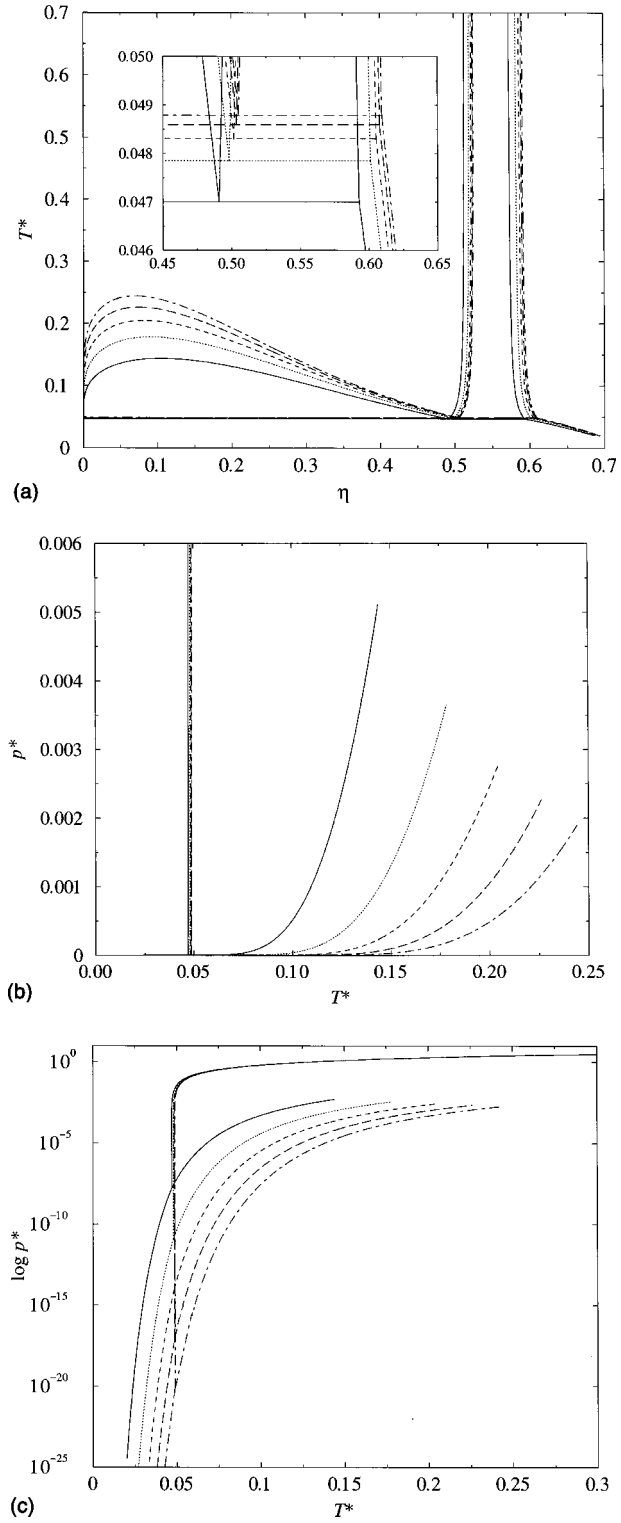

FIG. 3. (a) T-η, (b) p-T, and (c) $\log p$-T projections of the global phase diagram of fully flexible hard sphere chain molecules with segment–segment attractive interactions with lengths $m=2$ (solid curves), $m=3$ (dotted curves), $m=4$ (dashed curves), $m=5$ (long-dashed curves), and $m=6$ (dot-dashed curves). The inset in (a) shows the region close to the triple point.

phases are described with Wertheim's TPT1, so that flexible and linear rigid chains are described by the same equations in the fluid phase. This means that the vapor–liquid equilibria predicted by the theory for flexible and linear rigid chains are identical; although differences between the vapor–liquid equilibria of flexible and linear chains must exist, they are expected to be small. The p-T projection of the phase diagram is shown in Fig. 4(b). As can be seen, the solid–liquid coexistence pressure is greatly displaced toward higher temperatures as the chain length is increased, which suggests that the ordered solid phase of linear rigid chains is more stable than the disordered solid phase of fully flexible chain molecules. Another noticeable difference between both models is that the absolute values of the solid–vapor coexistence or sublimation pressure for linear rigid chains are several orders of magnitude larger than those corresponding to fully flexible chains of the same chain length. The low-temperature coexistence pressures can be seen more clearly in Fig. 4(c), in which a $\log p$-T representation is shown. As can be seen, the triple-point temperature and pressure increase as the chain length is increased, which clearly indicates that the ordered solid phase corresponding to linear rigid molecules becomes quite stable.

Let us now consider the phase diagrams of flexible and linear models in the case of very long chains. In Fig. 5 the phase diagram of the flexible model for longer chains is presented. As can be seen, the vapor–solid and fluid–solid equilibria are hardly affected by the length of the chain in this case (in agreement with our previous work[33]). This is a direct consequence of the scaling behavior of the Helmholtz free energy with the chain length.[28,33]

We have also studied the phase behavior of longer LTHS chains with segment–segment attractive interactions in order to determine the dependence of the triple-point temperature as the chain length is increased. However, care must be taken with these results. It is well known that LTHS chain molecules form liquid crystal phases for m longer than 5. One may suspect that the same must occur for rigid linear chains presenting attractive forces. Hence it is expected that the phase diagrams presented here for longer chains will be modified when the existence of liquid-crystalline phases is explicitly considered. Although beyond the scope of this work, it is possible that the commonly used lattice theory for liquid crystals could be incorporated in the Wertheim's formalism to deal with the liquid-crystalline phases exhibited by long LTHS chains. Unfortunately, it is not obvious to us how to extend the theoretical treatment of this work to deal with liquid-crystalline phases. Therefore, the results presented here for long linear rigid chains must be regarded with care and seen as only providing first hint of how the phase diagram would be in the absence of liquid-crystal phases.

The T-η and p-T projections of the phase diagram of linear chains for relatively long chain lengths are shown in Fig. 6. As can be seen in Fig. 6(a), the fluid densities at freezing move toward lower values as the chain length is increased, producing a shrinking of the fluid region. This is due to the stabilization of the solid phase with respect to the liquid phase. As a consequence, the triple-point temperature behaves completely different to that of the fully flexible chains: whereas in the flexible model the triple temperature is almost constant for the whole range of chain lengths considered, the triple temperature of linear rigid chains increases

TABLE III. Triple and critical temperatures of fully flexible hard sphere chains with segment–segment attractive interactions at the mean-field level of van der Waals. The liquid and solid densities (expressed in terms of packing fractions) at the triple point and the triple temperature to critical temperature ratio are also included.

m	T_c^*	T_t^*	η_s	η_l	T_t^*/T_c^*
2	0.143 92	0.046 99	0.592 81	0.490 90	0.326 50
3	0.178 44	0.047 85	0.601 07	0.498 20	0.268 16
4	0.204 91	0.048 30	0.605 21	0.501 68	0.235 71
5	0.226 32	0.048 59	0.607 69	0.503 72	0.214 69
6	0.244 24	0.048 79	0.609 35	0.505 12	0.199 76
8	0.273 04	0.049 04	0.611 41	0.506 69	0.179 61

for increasing molecular length, producing a wider range of temperatures in which the solid is in equilibrium with its vapor. In fact, a wide liquid–vapor temperature range is seen in the fully flexible models, while linear rigid chains formed by the same number of segments exhibit solid–vapor equilibria. For instance, a system of chains formed by seven tangent hard spheres with segment–segment attractive interactions at the mean-field level of van der Waals has a triple temperature to critical temperature ratio T_t/T_c, which is equal to 0.172 for the case of fully flexible chains, indicating a huge fluid range, and equal to 0.776 for linear molecules, indicating a narrow vapor–liquid coexistence. Note that this ratio increases toward the limiting case $T_t/T_c \rightarrow 1$ in which the vapor–liquid equilibria disappears because the solid phase becomes more stable that the liquid at all thermodynamic conditions. The prediction that the liquid range of linear rigid chains is quite small (i.e., high values of T_t/T_c) is somewhat surprising. For this reason, work is under way to determine by computer simulation the full phase diagram of linear rigid Lennard-Jones chains.[61] Preliminary results for $m=3$ and $m=5$ from simulation data confirm the trends predicted by the theory of this work.

Results corresponding to the solid–liquid, liquid–vapor, and solid–vapor coexistence pressures, as functions of temperature, for LTHS chains are shown in Fig. 6(b). As can be seen, a similar behavior to that corresponding to shorter chains is observed. The triple-point pressure of linear rigid chains increases as the chain length is increased, in agreement with the results for the T-η coexistence diagrams. In addition to the p-T projection of the phase diagram, we have also used a $\log p$-T representation in order to study the solid–vapor coexistence pressures with temperature. An increase of the chain length results in a displacement of the curve for the vapor–solid pressure toward higher temperatures. It is important to note that these pressures are several orders of magnitude higher than the pressures corresponding to fully flexible chains, as expected from previous results.

The differences between the global phase diagrams of fully flexible and linear rigid chains are a direct consequence of the differences between the free energies of both systems in the solid phase (in the present treatment the free energies of the fluid phase are identical, so that differences in the phase diagram arise from differences in the behavior of the solid phase). According to the theory of this work, differences in the free energy of the solid phase do not arise from the attractive forces (which in both cases are treated at the mean-field level), but rather in the treatment of the reference repulsive hard chain. In this respect the key equation to understand the different phase behavior of flexible and linear rigid chains is Eq. (14). Flexible chains can form a disordered solid whereas rigid chains cannot [as taken into account by the second parenthesis on the right-hand side of Eq. (14)]. When considering only the second term on the right-hand side of Eq. (14) it turns out that flexible chains should have lower free energy in the solid phase than linear rigid chains due to the presence of the degeneracy entropy. But this is only half of the history. Flexible and rigid chains differ not only in the type of solid they form, but more importantly, differ dramatically in the EOS of the solid phase, reflecting the important fact of having different Hamiltonians (to be flexible or to be rigid). Looking back, probably the surprising feature is not that flexible and linear rigid chains present different EOS in the solid phase, which can be attributed to the differences in the Hamiltonians of both models, but rather that they are so similar in the fluid phase (as can be seen from the simulation results of Figs. 1 and 2). Therefore, the key term to understand why the free energy of linear rigid chains is lower than that of flexible chains is the first term on the right-hand side of Eq. (14). The reduction in the number of degrees of freedom of the linear rigid chain [5 compared to $3+2(m-1)$] is responsible for the decrease of the compressibility factor and free energy of the linear rigid chain when compared to the flexible one. This reduction in the compressibility factor and free energy of a linear rigid chain with respect to the flexible chain is the key factor that determines the different phase diagram of flexible and rigid chains. The reduction in the free energy of the solid phase of linear rigid chains results in an additional stability of the solid phase and that moves the fluid densities at freezing to lower values.

Finally, we consider the phase diagram of longer LTHS chains with segment–segment attractive interactions at the mean-field level of van der Waals. The T-η projections of the phase diagram for molecules with chain lengths $m=11$, 12, 16, and 20 are shown in Fig. 7(a). As can be seen, the vapor–liquid coexistence becomes unstable for molecules formed by more than 11 tangent segments. (The triple and critical properties of a system formed by molecules with 11 linear rigid tangent segments are nearly identical; i.e., $T_t^*=0.297\,25$ and $p_t^*=0.835\,38\times10^{-3}$ and $T_c^*=0.305\,15$ and $p_c^*=0.999\,09\times10^{-3}$. See also Table IV for further details.) In other words, the vapor–liquid envelope lies below the vapor–solid coexistence curve, indicating that the vapor–

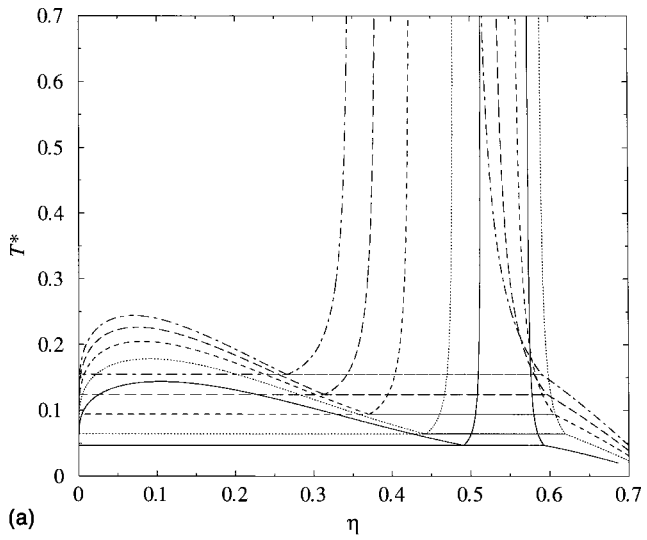

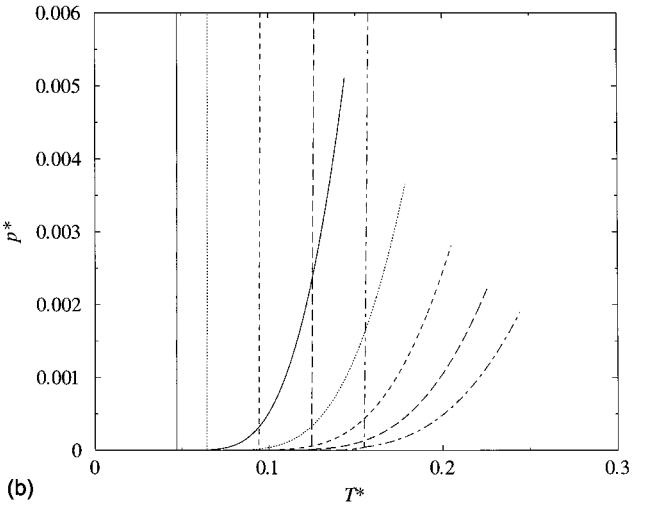

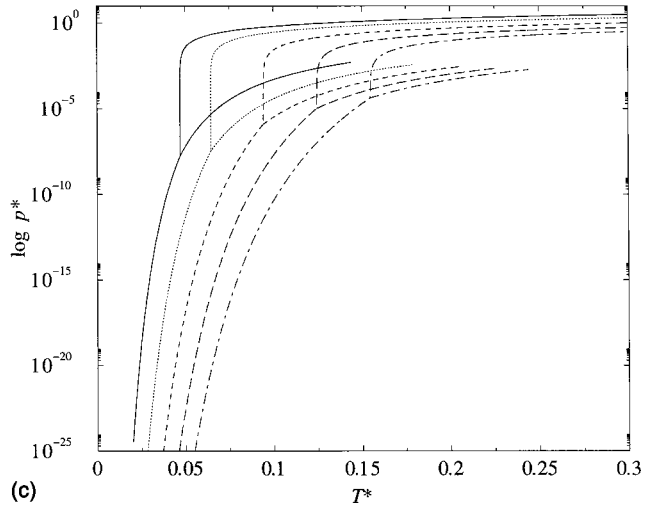

FIG. 4. (a) T-η, (b) p-T, and (c) $\log p$-T projections of the global phase diagram of LTHS chain molecules with segment–segment attractive interactions with lengths $m=3$ (dotted curves), $m=4$ (dashed curves), $m=5$ (long-dashed curves), and $m=6$ (dot-dashed curves). The phase behavior corresponding to dimers ($m=2$) is also included (solid curves).

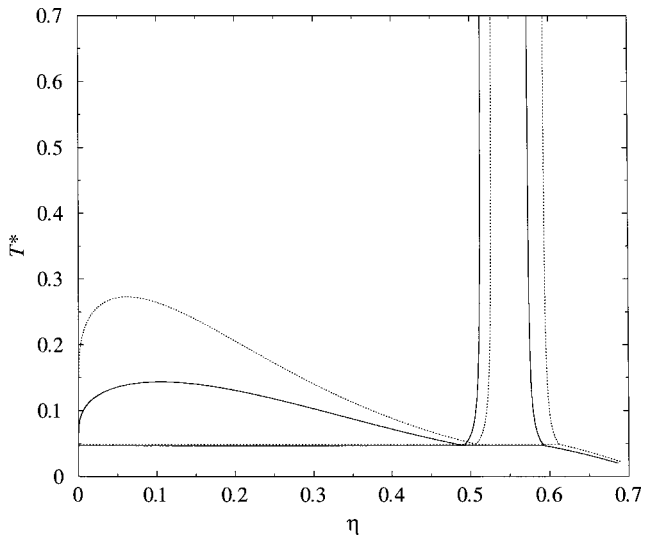

FIG. 5. T-η projection of the global phase diagram of fully flexible hard sphere molecules with segment–segment attractive interactions with lengths $m=2$ (solid curves) and $m=8$ (dotted curves).

liquid equilibria is metastable with respect to the solid phase. For longer chains, $m \geqslant 12$, linear rigid chains exhibit solid–fluid equilibria only. We have also obtained the coexistence pressure corresponding to the systems studied in Fig. 7(a). As can be seen in Fig. 7(b), the coexistence pressures move toward higher temperatures as the chain length is increased. A change in curvature is seen for a system formed by linear rigid chains with $m=12$ (and also for $m=16$, although with a lower change) in the region close to the critical region of chains with $m=11$, probably due to the presence of the metastable vapor–liquid coexistence. The extent of the fluid range for increasing chain lengths in the rigid and flexible models is summarized in Fig. 8. The calculated critical temperatures and triple temperatures [Fig. 8(a)] and the corresponding pressures [Fig. 8(b)] are considered. In these representations the disappearance of the fluid range for rigid chains longer than $m=11$ is suggested by the intersection of the curve of the critical points and the line of the triple points. The markedly different dependence of the triple-point conditions with increasing chain lengths in the rigid and flexible model is also highlighted. The triple-point temperatures increase linearly with increasing chain length in the case of the rigid model, while a close-to-constant behavior is found for the flexible model; in this case, the curves of critical and triple-point conditions do not intersect.

V. CONCLUSIONS

The global (solid–liquid, vapor–liquid, and solid–vapor) phase behavior of fully flexible and linear rigid hard sphere chains with segment–segment attractive interactions at the mean-field level of van der Waals has been obtained using Wertheim's first-order thermodynamic perturbation theory.

An extension of the original TPT1 theory of Wertheim has been proposed to describe the solid phase of linear rigid

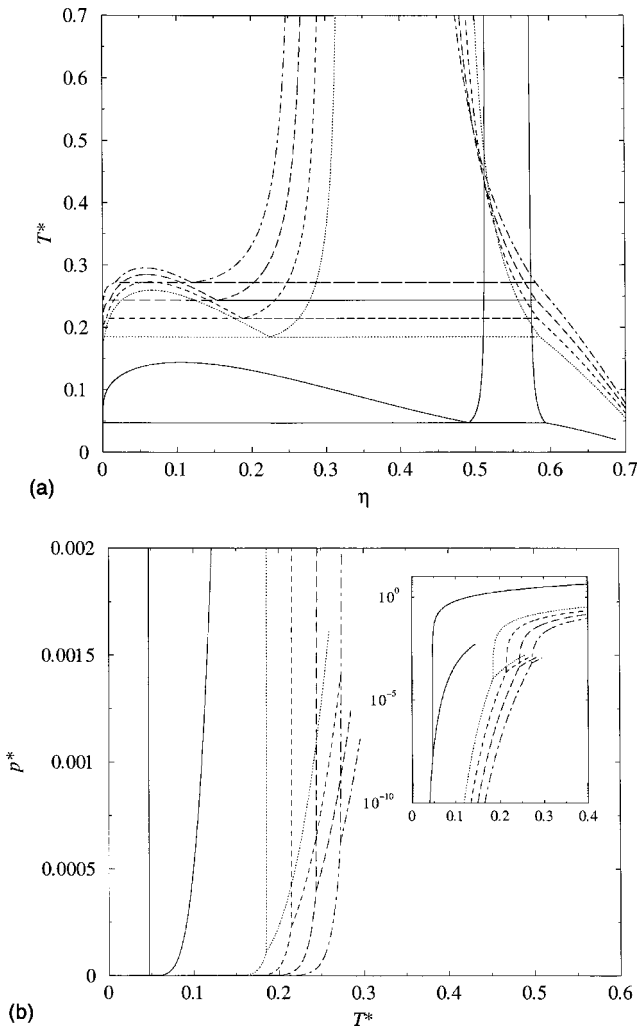

FIG. 6. (a) T-η and (b) p-T projections of the global phase diagram of LTHS chain molecules with segment-segment attractive interactions with lengths $m=7$ (dotted curves), $m=8$ (dashed curves), $m=9$ (long-dashed curves), and $m=10$ (dot-dashed curves). The phase behavior corresponding to dimers ($m=2$) is also included (solid curves). The inset of (b) also includes a log p-T representation of the coexistence pressure vs temperature.

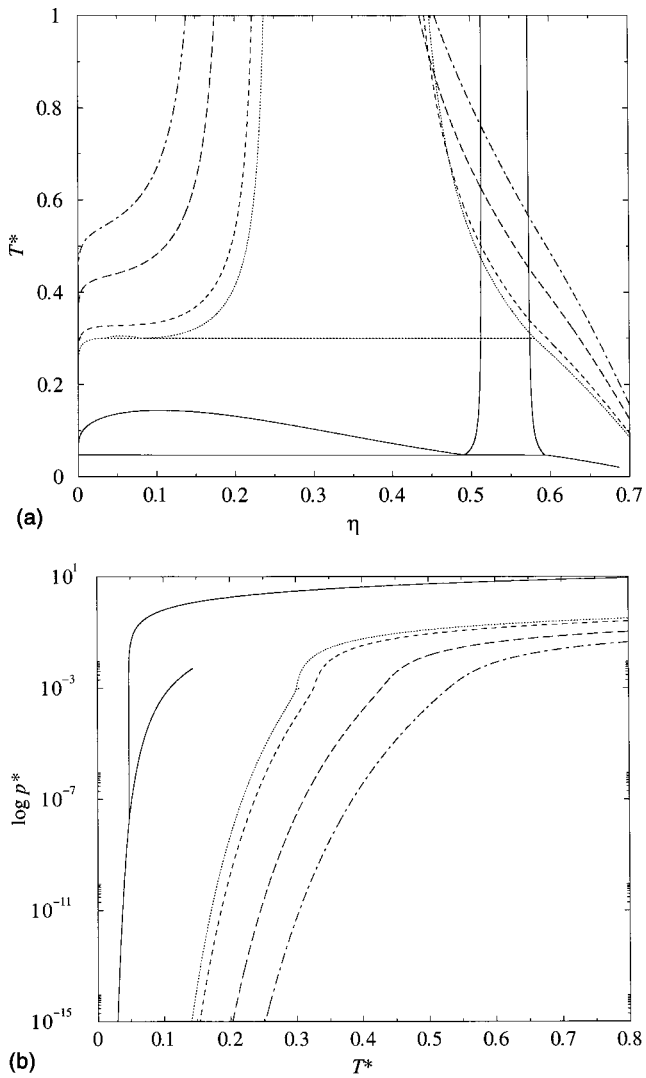

FIG. 7. (a) T-η projection and (b) log p-T representation of the global phase diagram of LTHS chain molecules with segment–segment attractive interactions with lengths $m=11$ (dotted curves), $m=12$ (dashed curves), $m=16$ (long-dashed curves), and $m=20$ (dot-dashed curves). The phase behavior corresponding to dimers ($m=2$) is also included (solid curves).

hard chain molecules. The theoretical framework, which is based on the scaling proposed recently by Vega and McBride,[42] provides an accurate description of the EOS of the system in the whole range of solid densities for different chain lengths. The scaling of the Helmholtz free energy takes into account explicitly the ordered nature of the solid structure corresponding to linear rigid chains.

In order to test the theoretical extension of the theory, we have determined by computer simulation (using the Einstein-crystal methodology) the Helmholtz free energy of LTHS chain molecules of three different chain lengths. This allowed the determination of the fluid–solid equilibrium of linear rigid chains with $m=3$ and 4. It has been found that the EOS and free energies of flexible and linear rigid chains are quite different in the solid phase. The theory proposed in this work provides a good description of the EOS and free energy for both flexible and linear rigid chains and is able to predict reasonably well the fluid–solid equilibrium of both models. It is striking that all that is needed to develop a theory for the fluid–solid equilibrium of hard sphere chains (flexible or rigid) is an EOS of hard sphere monomers in the fluid and in the solid phase.

The extension of Wertheim's perturbation theory is also used to study the phase behavior of linear chains with segment–segment attractive interactions treated at the mean-field level of van der Waals. In this sense the results presented here constitute the natural extension of the seminal work of Longuet-Higgins and Widom.[43,44]

The effect of increasing the chain length for linear rigid models is to move the coexistence densities of the fluid phase at freezing to lower values. The most noticeable effect of this behavior is the strong increase in the triple-point temperature and pressure as the chain length is increased. Due to this, the vapor–liquid coexistence region is greatly decreased. At temperatures below the triple point, the solid densities at coexistence move toward higher densities as the chain length is increased.

The behavior observed for LTHS chains is also compared with that corresponding to fully flexible molecules. In

TABLE IV. Triple-point properties of linear rigid hard chains with a mean-field attractive contribution as obtained from the extension of Wertheim's perturbation theory for the fluid and solid phases. The coexistence densities of the solid, liquid, and vapor phases at the triple point are denoted in terms of packing fractions η_s, η_l, and η_v, respectively. The critical pressure and temperature of the chains considered are also included.

m	T_t^*	p_t^*	T_c^*	p_c^*	η_s	η_l	η_v
3	0.064 40	$0.334\,49\times10^{-7}$	0.178 44	$0.365\,04\times10^{-2}$	0.619 44	0.441 93	$0.815\,87\times10^{-6}$
4	0.094 21	$0.127\,58\times10^{-5}$	0.204 91	$0.280\,89\times10^{-2}$	0.605 62	0.370 27	$0.283\,89\times10^{-4}$
5	0.124 44	$0.225\,43\times10^{-4}$	0.226 32	$0.227\,45\times10^{-2}$	0.596 50	0.313 34	$0.225\,34\times10^{-3}$
6	0.154 68	$0.424\,93\times10^{-4}$	0.244 24	$0.189\,82\times10^{-2}$	0.590 27	0.265 82	$0.884\,34\times10^{-3}$
7	0.184 68	$0.112\,34\times10^{-3}$	0.259 61	$0.161\,97\times10^{-2}$	0.586 01	0.224 71	$0.236\,84\times10^{-2}$
8	0.214 28	$0.230\,49\times10^{-3}$	0.273 04	$0.140\,89\times10^{-2}$	0.583 16	0.187 92	$0.508\,88\times10^{-2}$
9	0.243 38	$0.400\,40\times10^{-3}$	0.284 90	$0.124\,30\times10^{-2}$	0.581 36	0.153 68	$0.964\,03\times10^{-2}$
10	0.271 94	$0.621\,42\times10^{-3}$	0.295 52	$0.110\,90\times10^{-2}$	0.580 32	0.119 86	$0.173\,72\times10^{-1}$
11	0.299 94	$0.889\,22\times10^{-3}$	0.305 15	$0.999\,09\times10^{-3}$	0.579 88	0.079 88	0.034 23

the latter system, the solid–liquid and solid–vapor phase behavior is not very sensitive to chain length changes, and the phase boundaries reach very rapidly an asymptotic behavior as the chain length is increased. In particular, very small differences are observed for chains formed by more than four segments. Due to this behavior of the phase boundaries, the triple-point temperatures and pressures, as well as the critical properties, reach asymptotic limits.

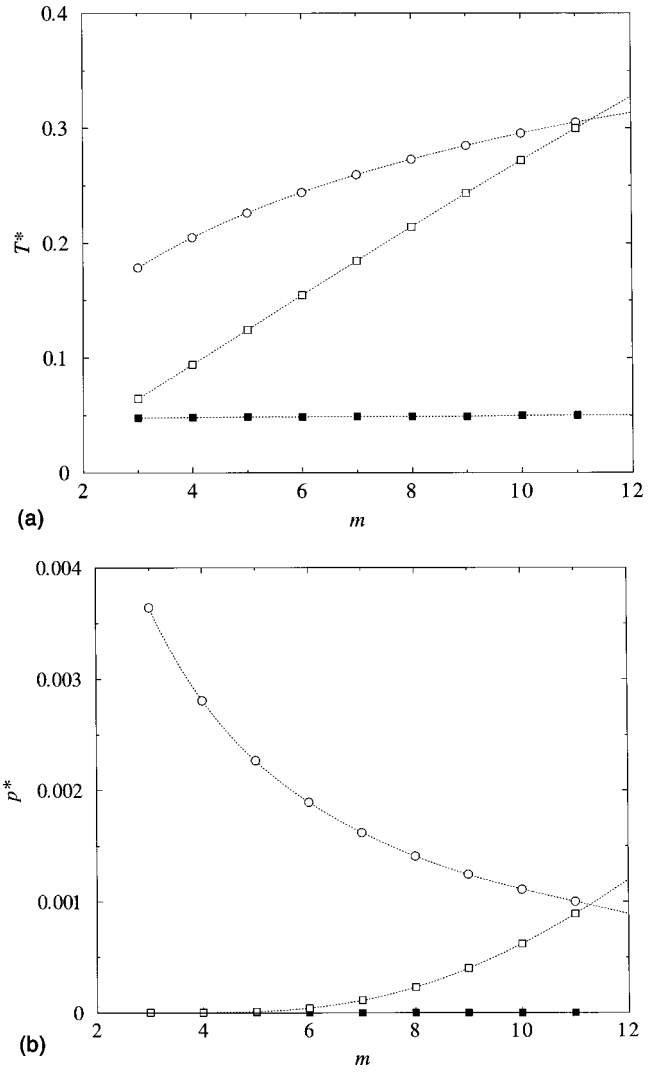

FIG. 8. Theoretical predictions for the critical and triple (a) temperatures and (b) pressures of fully flexible and linear rigid chains as functions of the chain length. The open circles represent the critical properties of fully flexible and linear rigid chains, the open squares the triple point properties of LTHS chains, and the solid squares the triple point properties of fully flexible molecules. The dotted curves are just guides to the eye.

The differences between the phase diagrams of fully flexible and linear rigid chain molecules are due to two factors: namely, the different type of solid they may form and the different scaling of the EOS and free energy of the solid phase that results from the difference in the Hamiltonian (one model is flexible while the other is rigid). Both contributions are accounted for in Eq. (14), although in an approximate way; this is probably one of the main contributions of this work. The different scaling means that for fully flexible chains the fluid–solid equilibrium is hardly affected by the length of the chains, whereas for the linear rigid model the fluid–solid equilibrium changes strongly with the length of the chain.

We have also considered long chain lengths in the linear rigid chain model in order to observe the effect of the stabilization effect of the solid phase on the vapor–liquid phase behavior. As the chains become larger, the solid–liquid boundaries move toward lower densities, making the vapor–liquid coexistence region smaller. For linear rigid chains formed by more than 11 segments, the solid phase becomes so stable with respect to the liquid that the vapor–liquid coexistence becomes unstable and no stable vapor–liquid equilibria is observed for $m>11$. In other words, for linear rigid chains with more than 11 segments, the system only exhibits solid–vapor phase behavior. Care must be taken, however, with respect to the results corresponding to these long linear rigid chains. It is well known that such a model, when only repulsions are taken into account, exhibits liquid-crystalline phases. Unfortunately, the simplified theoretical description presented here cannot be extended in a simple way to deal with liquid-crystalline phases. Here our aim was rather to illustrate a possible scenario of the phase diagram of flexible and linear rigid chains based on a simplified treatment. This work suggests that the analysis of the phase diagram of linear rigid chains may yield some surprises (extraordinary high values of T_t/T_c and, therefore, very small liquid ranges). This is certainly a problem which would be worth looking into in order to gain a better understanding of

the role of molecular flexibility on the global phase behavior of molecular chains.

ACKNOWLEDGMENTS

Financial support is due to project Nos. BFM-2001-1420-C02-01 and BFM-2001-1420-C02-02 of the Spanish DGICYT (Dirección General de Investigación Científica y Técnica). F.J.B. would like to acknowledge Universidad de Huelva and Junta de Andalucía for additional financial support. E.S. would like to thank the Ministerio de Educación y Cultura for the award of a PhD studentship (FPU). A.G. also thanks the Engineering and Physical Sciences Research Council for the award of an Advanced Research Fellowship.

[1] *Equations of State for Fluids and Fluid Mixtures*, edited by J. V. Senders, R. F. Kayser, C. J. Peters, and H. J. White, Jr. (Elsevier, Amsterdam, 2000).
[2] P. A. Monson and D. A. Kofke, Adv. Chem. Phys. **115**, 113 (2000).
[3] A. Z. Panagiotopoulos, Mol. Phys. **61**, 813 (1987).
[4] A. Lofti, J. Vrabec, and J. Fischer, Mol. Phys. **76**, 1319 (1992).
[5] D. A. Kofke, Mol. Phys. **78**, 1331 (1993).
[6] D. A. Kofke, J. Chem. Phys. **98**, 4149 (1993).
[7] M. Parrinello and A. Rahman, Phys. Rev. Lett. **45**, 1196 (1980).
[8] S. Yashonath and C. N. R. Rao, Mol. Phys. **54**, 245 (1985).
[9] D. Frenkel and A. J. C. Ladd, J. Chem. Phys. **81**, 3188 (1984).
[10] M. S. Wertheim, J. Stat. Phys. **35**, 19 (1984).
[11] M. S. Wertheim, J. Stat. Phys. **35**, 35 (1984).
[12] M. S. Wertheim, J. Stat. Phys. **42**, 459 (1986).
[13] M. S. Wertheim, J. Stat. Phys. **42**, 477 (1986).
[14] M. S. Wertheim, J. Chem. Phys. **85**, 2929 (1986).
[15] W. G. Chapman, G. Jackson, and K. E. Gubbins, Mol. Phys. **65**, 1057 (1988).
[16] W. G. Chapman, K. E. Gubbins, G. Jackson, and M. Radosz, Fluid Phase Equilib. **52**, 31 (1989).
[17] W. G. Chapman, K. E. Gubbins, G. Jackson, and M. Radosz, Ind. Eng. Chem. Res. **29**, 1709 (1990).
[18] W. G. Chapman, J. Chem. Phys. **93**, 4299 (1990).
[19] J. K. Johnson, E. A. Müller, and K. E. Gubbins, J. Phys. Chem. **98**, 6413 (1994).
[20] F. J. Blas and L. F. Vega, Mol. Phys. **92**, 135 (1997).
[21] F. J. Blas and L. F. Vega, J. Chem. Phys. **115**, 4355 (2001).
[22] L. G. MacDowell, M. Müller, C. Vega, and K. Binder, J. Chem. Phys. **113**, 419 (2000).
[23] A. Gil-Villegas, A. Galindo, P. J. Whitehead, S. J. Mills, G. Jackson, and A. N. Burgess, J. Chem. Phys. **106**, 4168 (1997).
[24] C. McCabe and G. Jackson, Phys. Chem. Chem. Phys. **1**, 2057 (1999).
[25] L. A. Davies, A. Gil-Villegas, and G. Jackson, J. Chem. Phys. **111**, 8659 (1999).
[26] E. A. Müller and K. E. Gubbins, *Equations of State for Fluids and Fluid Mixtures* (Elsevier, Amsterdam, 2000).
[27] E. A. Müller and K. E. Gubbins, Ind. Eng. Chem. Res. **40**, 2193 (2001).
[28] C. Vega and L. G. MacDowell, J. Chem. Phys. **114**, 10411 (2001).
[29] A. P. Malanoski and P. A. Monson, J. Chem. Phys. **107**, 6899 (1997).
[30] C. Vega, F. J. Blas, and A. Galindo, J. Chem. Phys. **116**, 7645 (2002).
[31] E. Sanz, C. McBride, and C. Vega, Mol. Phys. **101**, 2241 (2003).
[32] C. McBride and C. Vega, J. Chem. Phys. **116**, 1757 (2002).
[33] F. J. Blas, A. Galindo, and C. Vega, Mol. Phys. **101**, 449 (2003).
[34] C. Vega, C. McBride, E. de Miguel, F. J. Blas, and A. Galindo, J. Chem. Phys. **118**, 10696 (2003).
[35] K. W. Wojciechowski, A. C. Branka, and D. Frenkel, Physica A **196**, 519 (1993).
[36] K. W. Wojciechowski, D. Frenkel, and A. C. Branka, Phys. Rev. Lett. **66**, 3168 (1991).
[37] T. Boublík, C. Vega, and M. Díaz-Peña, J. Chem. Phys. **93**, 730 (1990).
[38] C. Vega, C. McBride, and L. G. MacDowell, J. Chem. Phys. **115**, 4203 (2001).
[39] C. Vega, E. P. A. Paras, and P. A. Monson, J. Chem. Phys. **96**, 9060 (1992).
[40] J. M. Polson and D. Frenkel, J. Chem. Phys. **109**, 318 (1998).
[41] J. M. Polson and D. Frenkel, J. Chem. Phys. **111**, 1501 (1999).
[42] C. Vega and C. McBride, Phys. Rev. E **65**, 052501 (2002).
[43] H. C. Longuet-Higgbins and B. Widom, Mol. Phys. **8**, 549 (1964).
[44] H. C. Longuet-Higgbins and B. Widom, Mol. Phys. **100**, 23 (2002).
[45] E. A. Paras, C. Vega, and P. A. Monson, Mol. Phys. **79**, 1063 (1993).
[46] N. F. Carnahan and K. E. Starling, J. Chem. Phys. **51**, 635 (1969).
[47] J. M. Polson, E. Trizac, S. Pronk, and D. Frenkel, J. Chem. Phys. **112**, 5339 (2000).
[48] K. R. Hall, J. Chem. Phys. **57**, 2252 (1972).
[49] R. J. Buehler, R. H. Wentorf, Jr., J. O. Hirschfelder, and C. F. Curtis, J. Chem. Phys. **19**, 61 (1950).
[50] J. E. Lennard-Jones and A. F. Devonshire, Proc. R. Soc. London, Ser. A **163**, 53 (1937).
[51] A. R. Denton, N. W. Ashcroft, and W. A. Curtin, Phys. Rev. E **51**, 65 (1995).
[52] R. Dickman and C. K. Hall, J. Chem. Phys. **89**, 3168 (1988).
[53] A. Hertanto and R. Dickman, J. Chem. Phys. **89**, 7577 (1988).
[54] P. J. Flory, J. Chem. Phys. **9**, 660 (1941).
[55] M. L. Huggins, J. Chem. Phys. **9**, 440 (1941).
[56] D. Frenkel and B. M. Mulder, Mol. Phys. **55**, 1171 (1985).
[57] C. Vega and P. A. Monson, J. Chem. Phys. **102**, 1361 (1995).
[58] E. de Miguel and C. Vega, J. Chem. Phys. **117**, 6313 (2002).
[59] C. Vega, S. Lago, and B. Garzon, Mol. Phys. **82**, 1233 (1994).
[60] D. C. Williamson and G. Jackson, J. Chem. Phys. **108**, 10294 (1998).
[61] A. Galindo, C. Vega, E. Sanz, L. G. MacDowell, E. de Miguel, and F. J. Blas, J. Chem. Phys. (to be published).